

1 Greenhouse gas fluxes in mangrove forest soil in an Amazon estuary

2 Saúl Edgardo Martínez Castellón¹, José Henrique Cattanio^{1*}, José Francisco Berrêdo^{1;3},
3 Marcelo Rollnic², Maria de Lourdes Ruivo^{1;3}, Carlos Noriega².

4 ¹ Graduate Program in Environmental Sciences. Federal University of Pará, Belém,
5 Brazil

6 ² Marine Environmental Monitoring Research Laboratory. Federal University of Pará,
7 Belém, Brazil.

8 ³ Department of Earth Sciences and Ecology. Paraense Emílio Goeldi Museum, Belém,
9 Brazil

10 * Corresponding author: cattanio@ufpa.br (J.H. Cattanio)

11 Abstract: Tropical mangrove forests are important carbon sinks, the soil being the main
12 carbon reservoir. Understanding the variability and the key factors that control fluxes is
13 critical to accounting for greenhouse gas (GHG) emissions, particularly in the current
14 scenario of global climate change. This study is the first to quantify methane (CH₄) and
15 carbon dioxide (CO₂) emissions using a dynamic chamber in a natural mangrove soil of
16 the Amazon. The plots for the trace gases study were allocated at contrasting
17 topographic heights. The results showed that the mangrove soil of the Amazon estuary
18 is a source of CO₂ (6.66 g CO₂ m⁻² d⁻¹) and CH₄ (0.13 g CH₄ m⁻² d⁻¹) to the atmosphere.
19 The CO₂ flux was higher in the high topography (7.858 g CO₂ m⁻² d⁻¹) than in the low
20 topography (4.734 g CO₂ m⁻² d⁻¹) in the rainy season, and CH₄ was higher in the low
21 topography (0.128 g CH₄ m⁻² d⁻¹) than in the high topography (0.014 g CH₄ m⁻² d⁻¹) in
22 the dry season. However, in the dry period, the low topography soil produced more
23 CH₄. Soil organic matter, carbon and nitrogen ratio (C/N), and redox potential
24 influenced the annual and seasonal variation of CO₂ emissions; however, they did not
25 affect CH₄ flux. The mangrove soil of the Amazon estuary produced 35.4 Mg CO₂-eq ha⁻¹
26 y⁻¹. A total of 2.16 kg CO₂ m⁻² y⁻¹ needs to be sequestered by the mangrove ecosystem
27 to counterbalance CH₄ emissions.

28 1 Introduction

29 The mangrove areas are estimated to be the main contributors to greenhouse gas
30 emissions in marine ecosystems (Allen et al., 2011; Chen et al., 2012). However,
31 mangrove forests are highly productive due to a high nutrient turnover rate (Robertson
32 et al., 1992) and have mechanisms that maximize carbon gain and minimize water loss
33 through plant transpiration (Alongi and Mukhopadhyay, 2015). A study conducted in 25
34 mangrove forests (between 30° latitude and 73° longitude) revealed that these forests

35 are the richest in carbon storage in the tropics, containing on average 1,023 Mg C ha⁻¹ of
36 which 49 to 98% is present in the soil (Donato et al., 2011).

37 The estimated soil CO₂ outgassing, in tropical estuarine areas is 16.2 Tg C y⁻¹ (Alongi,
38 2009). However, soil efflux measurements from tropical mangroves revealed emissions
39 ranging from 2.9 to 11.0 g CO₂ m⁻² d⁻¹ (Castillo et al., 2017; Chen et al., 2014; Shiau
40 and Chiu, 2020). In situ CO₂ production is related to the water input of terrestrial,
41 riparian, and groundwater brought by rainfall (Rosentreter et al., 2018b). Due to the
42 periodic tidal movement, the mangrove ecosystem is daily flooded, leaving the soil
43 anoxic and consequently reduced, favoring methanogenesis (Dutta et al., 2013). Thus,
44 estuaries are considered hotspots for CH₄ production and emission (Bastviken et al.,
45 2011; Borges et al., 2015). The organic material decomposition by methanogenic
46 bacteria in anoxic environments, such as sediments, inner suspended particles,
47 zooplankton gut (Reeburgh, 2007; Valentine, 2011), and the impact of freshwater
48 should change the electron flow from sulfate-reducing bacteria to methanogenesis
49 (Purvaja et al., 2004), which also results in CH₄ formation. On the other hand, an
50 ecosystem with salinity levels above 18 ppt may show an absence of CH₄ emissions
51 (Poffenbarger et al., 2011), since methane dissolved in pores is typically oxidized
52 anaerobically by sulfate (Chuang et al., 2016). Currently the uncertainty in emitted CH₄
53 values in vegetated coastal wetlands is approximately 30% (EPA, 2017). Soil flux
54 measurements from tropical mangroves revealed emissions ranging from 0.3 to 4.4 mg
55 CH₄ m⁻² d⁻¹ (Castillo et al., 2017; Chen et al., 2014; Kreuzwieser et al., 2003).

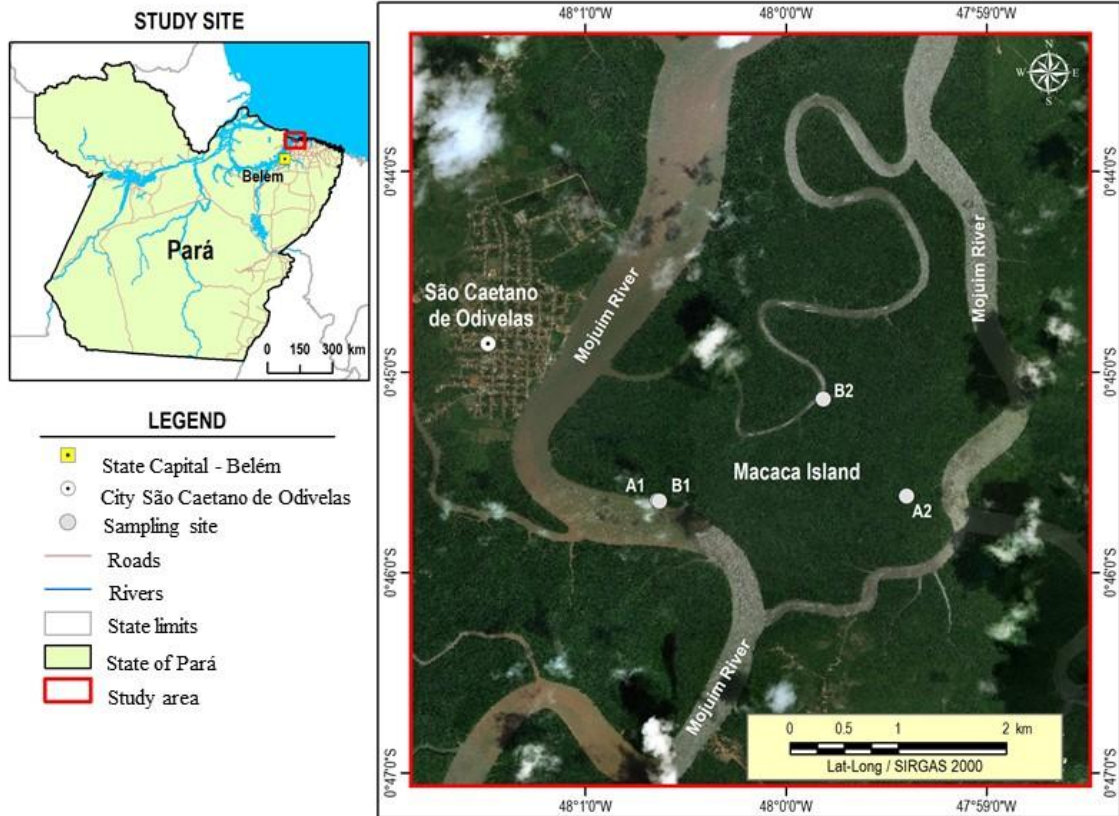
56 The production of greenhouse gases from soils is mainly driven by biogeochemical
57 processes. Microbial activities and gas production are related to soil properties,
58 including total carbon and nitrogen concentrations, moisture, porosity, salinity, and
59 redox potential (Bouillon et al., 2008; Chen et al., 2012). Due to the dynamics of tidal
60 movements, mangrove soils may become saturated and present a reduced oxygen
61 availability, or suffer total aeration caused by the ebb tide. Studies attribute soil carbon
62 flux responses to moisture perturbations because of seasonality and flooding events
63 (Banerjee et al., 2016), with fluxes being dependent on tidal extremes (high tide and low
64 tide), and flood duration (Chowdhury et al., 2018). In addition, phenolic compounds
65 inhibit microbial activity and help keep organic carbon intact, thus leading to the
66 accumulation of organic matter in mangrove forest soils (Friesen et al., 2018).

67 The Amazonian coastal areas in the State of Pará (Brazil) cover 2,176.8 km² where
68 mangroves develop under the macro-tide regime (Souza Filho, 2005), representing
69 approximately 85% of the entire area of Brazilian mangroves (Herz, 1991). The
70 objective of this study is to investigate the monthly flux of CO₂ and CH₄ from the soil,
71 at two topographic heights, in a pristine mangrove area in the Mojuim River Estuary,
72 belonging to the Amazon biome. The gas fluxes were studied together with the analysis
73 of the vegetation structure and soil physical-chemical parameters.

74 **2 Material and Methods**

75 **2.1 Study site**

76 This study was conducted in the Amazonian coastal zone, Macaca Island (-0.746491
77 latitude and -47.997219 longitude), located in the Mojuim River estuary, at the
78 Mocapajuba Marine Extractive Reserve, municipality of São Caetano de Odivelas
79 (Figure 1), state of Pará (Brazil). The Macaca island has an area of 1,322 ha of pristine
80 mangroves, which belongs to a mangrove area of 2,177 km² in the state of Pará (Souza
81 Filho, 2005). The climate is type Am (tropical monsoon) according to the Köppen
82 classification (Peel et al., 2007). The climatological data were obtained from the
83 Meteorological Database for Teaching and Research of the National Institute of
84 Meteorology (INMET). The area has a rainy season from January to June (2,296 mm of
85 precipitation) and a dry season from July to December (687 mm). March and April were
86 the rainiest months with 505 and 453 mm of precipitation, while October and November
87 were the driest (53 and 61 mm, respectively). The minimum temperatures occur in the
88 rainy period (26 °C) and the maximum in the dry period (29 °C). The Mojuim estuary
89 has a macrotidal regime, with an average amplitude of 4.9 m during spring tide and 3.2
90 m during low tide (Rollnic et al., 2018). During the wet season the Mojuim River has a
91 flow velocity of 1.8 m s⁻¹ at the ebb tide and 1.3 m s⁻¹ at the flood tide. During the dry
92 season, the maximum currents reach 1.9 m s⁻¹ at the flood and 1.67 m s⁻¹ at the ebb tide
93 (Rocha, 2015). The annual mean salinity is 26.95 PSU (Valentim et al., 2018).



94

95 Figure 1. The Macaca Island located in the mangrove coast of Northern Brazil,
 96 Municipality of São Caetano de Odivelas (state of Pará), with sampling points at low
 97 (plot B1 and plot B2) and high topographies (plot A1 and plot A2). Image Source: ©
 98 Google Earth

99 The Mojuim River region is geomorphologically formed by partially submerged river
 100 basins consequent of the increase in the relative sea level during the Holocene (Prost et
 101 al., 2001) associated with the formation of mangroves, dunes, and beaches (El-Robrini
 102 et al., 2006). This river forms the entire watershed of the municipality of São Caetano
 103 de Odivelas and borders the municipality of São João da Ponta (Figure 1). Before
 104 reaching the estuary, the Mojuim River crosses an area of a dryland forest highly
 105 fragmented by family farming, forming remnants of secondary forest (< 5.0 ha) of
 106 various ages (Fernandes and Pimentel, 2019). The population economically exploited
 107 the estuary, primarily by artisanal fishing, crab (*Ucides cordatus* L.) extraction, and
 108 oyster farms.

109 The flora of the mangrove area of Macaca Island is little anthropized and comprises the
 110 plant genera *Rhizophora*, *Avicenia*, *Laguncularia*, and *Acrostichum* (Ferreira, 2017;
 111 França et al., 2016). The estuarine plains are influenced by macrotide dynamics and can

112 be physiographically divided into four sectors (França et al., 2016). The Macaca Island
113 is ranked as being from the fourth sector, which implies having woods of adult trees of
114 the genus *Ryzophora* with an average height of 10 to 25 m, being located at an elevation
115 of 0 to 5 m, and having silt-clay soil (França et al., 2016).

116 Four sampling plots were selected in the Macaca Island (Figure 1) on 19/05/2017, when
117 the moon was in the waning quarter phase: two plots where flooding occurs every day
118 (plots B1 and B2; Figure 1), called low topography (Top_Low), and two plots where
119 flooding occurs only at high tides during the solstice and on the high tides of the rainy
120 season of the new and full moons (plots A1 and A2; Figure 1), called high topography
121 (Top_High).

122 2.2 Greenhouse gas flux measurements

123 In each plot, eight Polyvinyl Chloride rings with 0.20 m diameter and 0.12 m height
124 were randomly installed within a circumference with a diameter of 20 m. The rings had
125 an area of 0.028 m² (volume of 3.47 L), were fixed 0.05 m into the ground, and
126 remained in place until the study was completed. Once a month, the Greenhouse gas
127 flux was measured during periods of waning or crescent moon, as these are the times
128 when the soil in the low topography is more exposed. To avoid the influence of
129 mangrove roots on the gas fluxes, the rings were placed in locations without any
130 seedlings or aboveground mangrove roots. CO₂ and CH₄ concentrations (ppm) were
131 measured using the dynamic chamber methodology (Norman et al., 1997; Verchot et al.,
132 2000), sequentially connected to a Los Gatos Research portable gas analyzer (Mahesh et
133 al., 2015). The device was calibrated monthly with a high quality standard gas (500 ppm
134 CO₂; 5 ppm CH₄). The rings were sequentially closed for three minutes with a PVC cap,
135 being connected to the analyzer through two 12.0 m polyethylene hoses. The gas
136 concentration was measured every two seconds and automatically stored by the
137 analyzer. CO₂ and CH₄ fluxes were calculated from the linear regression of
138 increasing/decreasing CO₂ and CH₄ concentrations within the chamber, usually between
139 one and three minutes after the ring cover was placed (Frankignoulle, 1988; McEwing
140 et al., 2015). The flux is considered zero when the linear regression reaches an R² <
141 0.30 (Sundqvist et al., 2014). However, in our analyses, most regressions reached R² >
142 0.70, and the regressions were weak and considered zero in only 6% of the samples. At
143 the end of each flux measurement, the height of the ring above ground was measured at

144 four equidistant points with a ruler. The seasonal data were analyzed by comparing the
145 average monthly fluxes in the wet season and dry season separately.

146 **2.3 Vegetation structure and biomass**

147 The floristic survey was conducted in October 2017 using circular 1,256.6 m² plots
148 (Kauffman et al., 2013) divided into four 314.15 m² subplots, which is the equivalent to
149 0.38 ha (Figure 1), at the same topographies as the gas flux analysis. We recorded the
150 diameter above the aerial roots, the diameter of the stem, and total height of all trees
151 with DBH (diameter at breast height; m) greater than 0.05m. The allometric equations
152 (Howard et al., 2014) to calculate tree biomass (aboveground biomass; AGB) were:
153 $AGB = 0.1282 * DBH^{2.6}$ ($R^2 = 0.92$) for *R. mangle*; $AGB = 0.140 * DBH^{2.4}$ ($R^2 = 0.97$)
154 for *A. germinans*; and $Total\ AGB = 0.168 * \rho * DBH^{2.47}$ ($R^2 = 0.99$), where $\rho_{R. mangle} =$
155 0.87 ; $\rho_{A. germinans} = 0.72$ ($\rho =$ wood density).

156 **2.4 Soil sampling and environmental characterization**

157 Four soil samples were collected with an auger at a depth of 0.10 m in all the studied
158 plots for gas flux measurements in July 2017 (beginning of the dry season) and January
159 2018 (beginning of the rainy season; Figure 1). Before the soil samples were removed,
160 pH and redox potential (Eh; mV) were measured with a Metrohm 744 equipment by
161 inserting the platinum probe directly into the intact soil at a depth of 0.10 m (Bauza et
162 al., 2002). The soil samples collected in the field were transported to the laboratory
163 (Chemical Analysis Laboratory of the *Museu Paraense Emílio Goeldi*) in thermal boxes
164 containing ice. The soil samples were analyzed on the day after collection at the
165 laboratory, and the samples were kept in a freezer. Salinity (Sal; ppt) was measured with
166 PCE-0100, and soil moisture (Sm; %) by the residual gravimetric method (EMBRAPA,
167 1997).

168 Organic Matter (OM; g kg⁻¹), Total Carbon (T_C; g kg⁻¹) and Total Nitrogen (T_N; g kg⁻¹)
169 were calculated by volumetry (oxidoreduction) using the Walkley-Black method
170 (Kalembasa and Jenkinson, 1973). Microbial carbon (C_{mic}; mg kg⁻¹) and microbial
171 nitrogen (N_{mic}; mg kg⁻¹) were determined through the 2.0 min of Irradiation-extraction
172 method of soil by microwave technique (Islam and Weil, 1998). Microwave heated soil
173 extraction proved to be a simple, fast, accurate, reliable, and safe method to measure
174 soil microbial biomass (Araujo, 2010; Ferreira et al., 1999; Monz et al., 1991). The C_{mic}
175 was determined by dichromate oxidation (Kalembasa and Jenkinson, 1973; Vance et al.,

176 1987). The N_{mic} was analyzed following the method described by Brookes et al. (1985),
177 changing fumigation to irradiation, which uses the difference between the amount of T_N
178 in irradiated and non-irradiated soil. We used the flux conversion factor of 0.33
179 (Sparling and West, 1988) and 0.54 (Almeida et al., 2019; Brookes et al., 1985), for
180 carbon and nitrogen, respectively. Particle size analysis was performed separately on
181 four soil samples collected at each flux plot, in the two seasons (October 2017 and
182 March 2018), according to EMBRAPA (1997).

183 At each gas flux measurement, environmental variables such as air temperature (T_{air} ,
184 °C), relative humidity (RH, %), and wind speed (W_s , $m\ s^{-1}$) were quantified with a
185 portable thermo-hygrometer (model AK821) at the height of 2.0 m above the soil
186 surface. Soil temperature (T_s , °C) was measured with a portable digital thermometer
187 (model TP101) after each gas flux measurement. Daily precipitation was obtained from
188 an automatic precipitation station installed at a pier on the banks of the Mojuim River in
189 São Caetano das Odivelas (coordinates: -0.738333 latitude; -48.013056 longitude).

190 2.5 Statistical analyses

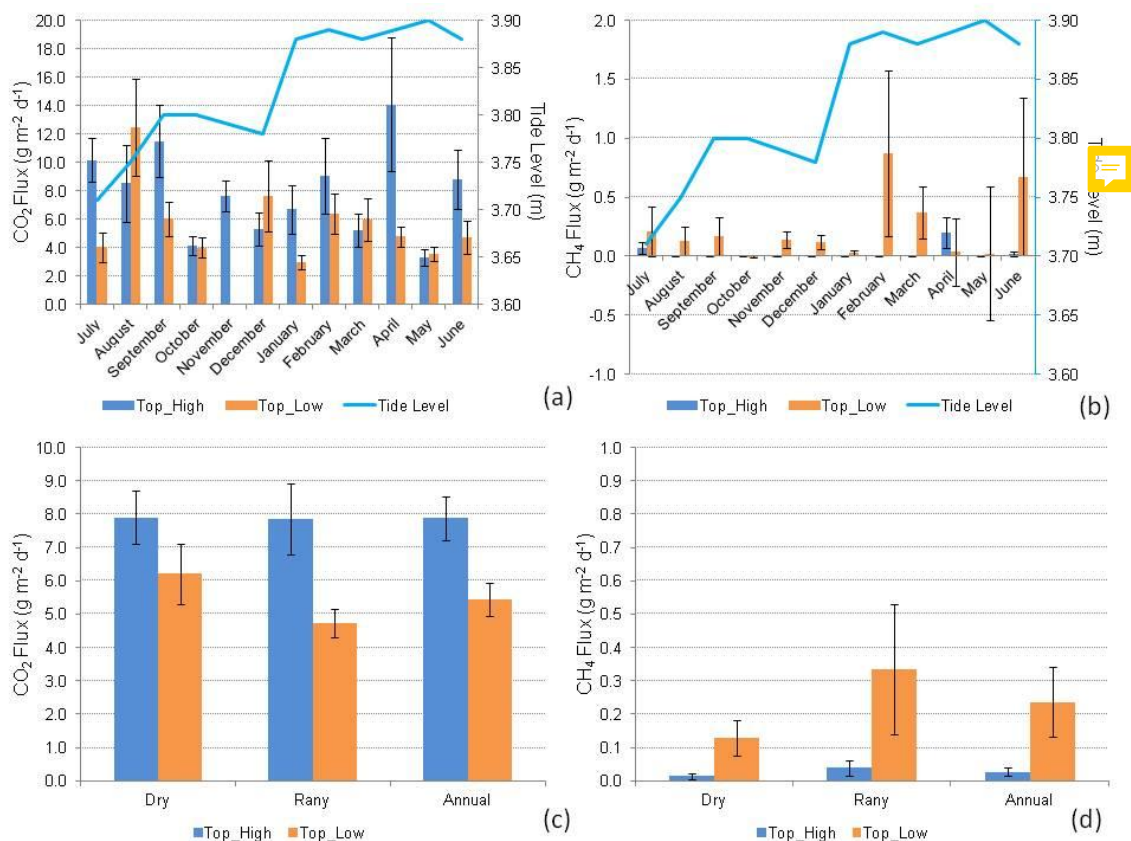
191 On the Macaca Island, two treatments were allocated (low and high topography), with
192 two plots in either. In each plot, eight chambers were randomly distributed, which were
193 considered sample repetitions. The normality of the data of FCH_4 , F_{CO_2} , and soil
194 physicochemical parameters was evaluated using the Shapiro-Wilks method. The soil
195 CO_2 and CH_4 flux showed a non-normal distribution. Therefore, we used the non-
196 parametric ANOVA (Kruskal-Wallis, $p < 0.05$) to test the differences between the two
197 treatments among months and seasons. The physicochemical parameters were normally
198 distributed. Therefore, a parametric ANOVA was used to test the statistical differences
199 ($p < 0.05$) between the two treatments among months and seasons. Pearson correlation
200 coefficients were calculated to determine the relationships between soil properties and
201 gas fluxes in the months (dry and wet season) when the chemical properties of the soil
202 were analyzed at the same time as gas fluxes were measured. Statistical analyses were
203 performed with the free statistical software Infostat 2015®.

204 3 Results

205 3.1 Carbon dioxide and methane fluxes

206 CO_2 fluxes differed significantly between topographies only in January ($H = 3.915$; $p =$
207 0.048), July ($H = 9.091$; $p = 0.003$), and November ($H = 11.294$; $p < 0.000$) (Figure 2;

208 Supplementary Information, SI 1), with generally higher fluxes at the high topography
 209 than at the low topography. At the high topography, CO₂ fluxes were significantly
 210 higher (H = 24.510; p = 0.011) in July compared to August and December, March,
 211 October, and May, not differing from the other months of the year. Similarly, at the low
 212 topography, CO₂ fluxes were statistically higher (H = 19.912; p = 0.046) in September
 213 and February than in January and November, not differing from the other months. We
 214 found a mean monthly flux of 327.9 ± 78.0 mg CO₂ m⁻² h⁻¹ (mean ± standard error) and
 215 217.2 ± 51.0 mg CO₂ m⁻² h⁻¹ at the high and low topographies, respectively.



216

217 **Figure 2.** CO₂ (a) and CH₄ (b) fluxes (g CO₂ or CH₄ m⁻² d⁻¹) monthly (July 2018 to June
 218 2019) (n = 16). Seasonal (Dry and Rany) and annual fluxes of CO₂ (c) and CH₄ (d), at
 219 high (Top_High) and low (Top_Low) topographies (n = 96), in a mangrove forest soil
 220 compared to tide level (Tide Level). The bars represent the standard error of the mean.

221 The CH₄ fluxes were statistically different between topographies only in November (H
 222 = 9.276; p = 0.002) and December (H = 4.945; p = 0.005), with higher fluxes at the low
 223 topography (Figure 2; SI 1). At the high topography, CH₄ fluxes were significantly (H =
 224 40.073; p < 0.001) higher in April and July compared to the other months studied, and
 225 in November CH₄ was consumed from the atmosphere (Figure 2; SI 1). Similarly, CH₄

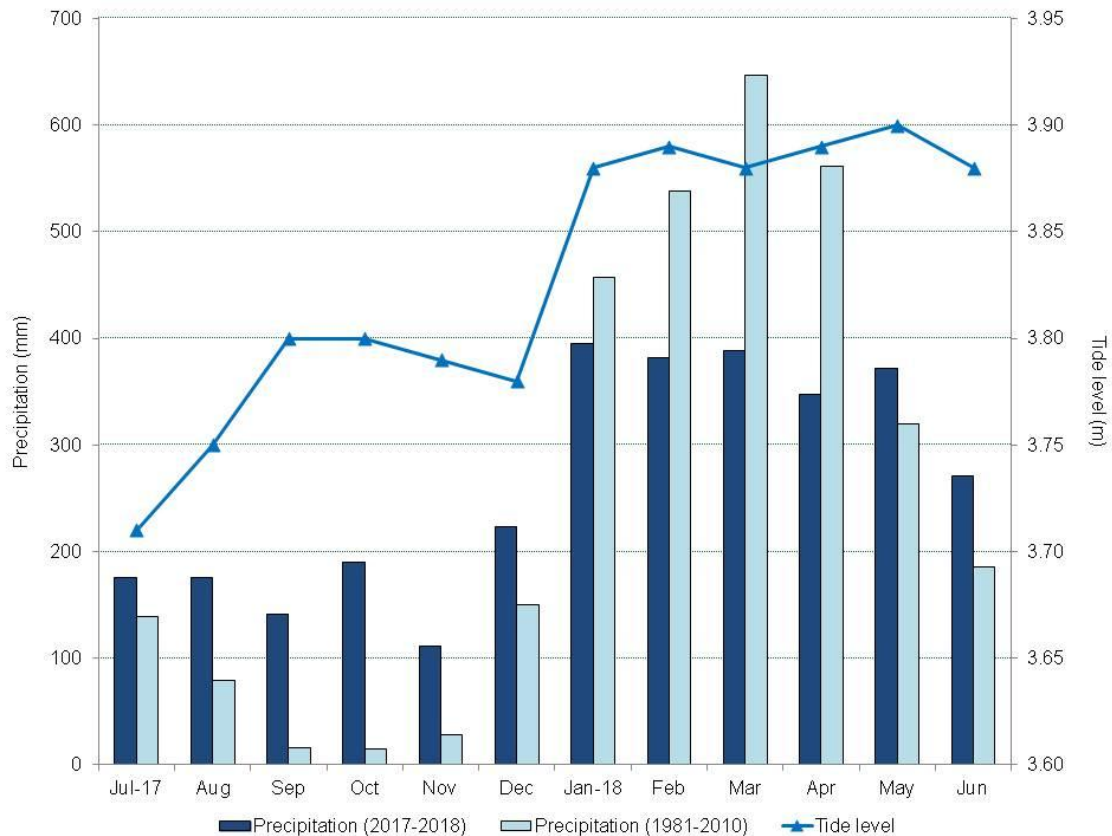
226 fluxes at the low topography did not vary significantly among months ($H = 10.114$; $p =$
227 0.407).

228 Greenhouse gas fluxes (Figure 2) were only significantly different between
229 topographies in the dry season (Figure 3), period when CO_2 fluxes were higher ($H =$
230 7.378 ; $p = 0.006$) at the high topography and CH_4 fluxes at the low topography ($H =$
231 8.229 ; $p < 0.001$). In the Macaca Island, the mean annual fluxes of CO_2 and CH_4 were
232 $6.659 \pm 0.419 \text{ g CO}_2 \text{ m}^{-2} \text{ d}^{-1}$ and $0.132 \pm 0.053 \text{ g CH}_4 \text{ m}^{-2} \text{ d}^{-1}$, respectively.

233 3.2 Weather data

234 There was a marked seasonality during the study period (Figure 2), with 2,155.0 mm of
235 precipitation during the rainy period and 1,016.5 mm during the dry period. The highest
236 tides occurred in the period of greater precipitation (Figure 3) due to the rains. However,
237 the rainfall distribution was different from the climatological normal (Figure 3). The
238 precipitation in the rainy season was 553.2 mm below and in the dry season was 589.1
239 mm above the climatological normal. Thus, in the period studied, the dry season was
240 rainier and the rainy season drier than the climatological normal, which may be a
241 consequence of global climate change.

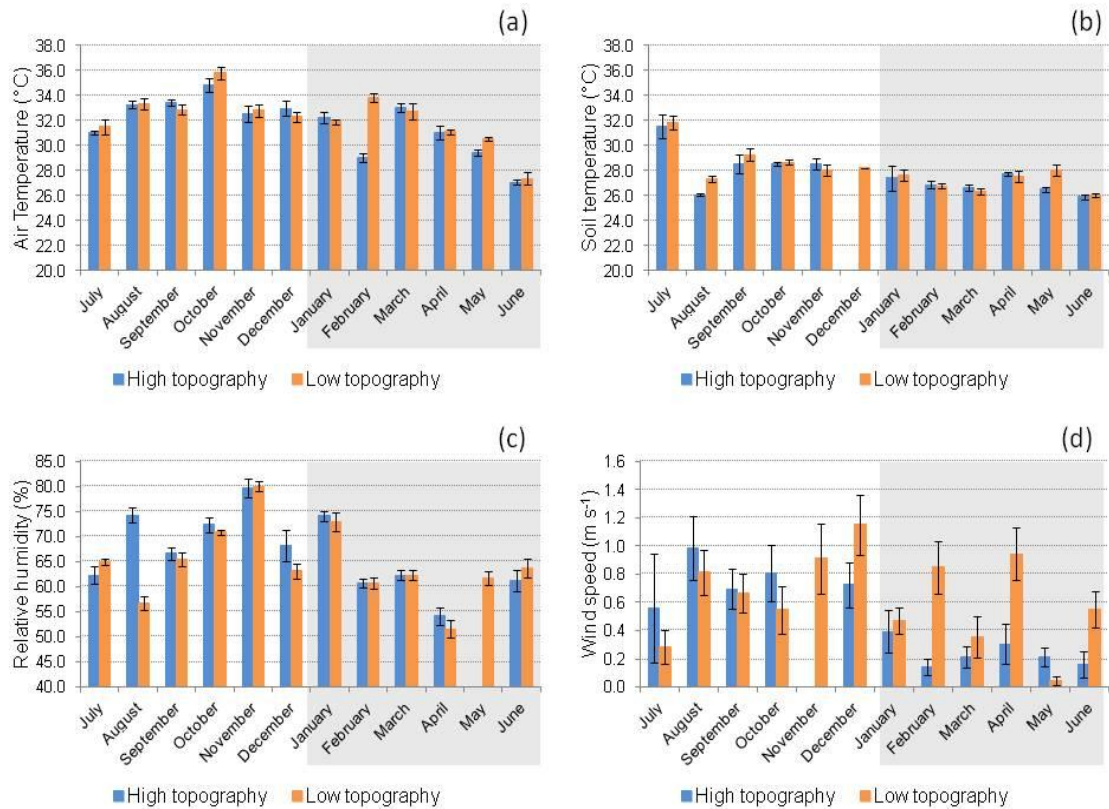
242



243

244 Figure 3. Monthly climatological normal in the municipality of Soure (1981-2010, mm),
 245 monthly precipitation (mm), and maximum tide height (m) from 2017 to 2018, in the
 246 municipality of São Caetano de Odivelas (PA).

247 T_{air} was significantly higher (LSD = 0.72, $p = 0.01$) at the high (31.24 ± 0.26 °C) than at
 248 the low topography (30.30 ± 0.25 °C) only in the rainy season (Figure 4a). No
 249 significant variation in T_s was found between topographies in either season (Figure 4b).
 250 RH was significantly higher (LSD = 2.55, $p = 0.01$) at the high topography ($70.54 \pm$
 251 0.97%) than at the low topography ($66.85 \pm 0.87\%$) only in the rainy season (Figure 4c).
 252 W_s (Figure 4d) was significantly higher (LSD = 0.15, $p < 0.00$) at the low (0.54 ± 0.06
 253 $m s^{-1}$) than at the high topography ($0.24 \pm 0.04 m s^{-1}$) also in the rainy season.



254

255 Figure 4. a) Air temperature (°C), b) soil temperature (°C), c) relative humidity (%), and
 256 d) wind speed (m s⁻¹) at high and low topographies, from July 2017 to June 2018 in a
 257 mangrove area in the Mojuim River estuary. Bars highlighted in grey correspond to the
 258 rainy season (n = 16). The bars represent the standard error.

259 3.3 Soil characteristics

260 Silt concentration was higher at the low topography (LSD: 14.763; p= 0.007) and clay
 261 concentration was higher at the high topography plots (LSD: 12.463; p= 0.005), in both
 262 seasons studied (Table 1). Soil particle size analysis did not differ statistically (p > 0.05)
 263 between the two seasons (Table 1). Soil moisture did not vary significantly (p > 0.05)
 264 between topographies at each season, or between seasonal periods at the same
 265 topography (Table 1). The pH varied statistically (LSD: 5.950; p= 0.006) only at the
 266 low topography when the two seasons were compared, being more acidic in the dry
 267 period (Table 1). The pH values were significantly (LSD: 0.559; p= 0.008) higher in the
 268 dry season (Table 1). No variation in Eh was identified between topographies and
 269 seasons (Table 1), although it was higher in the dry season than in the rainy season.
 270 However, Sal values were higher (LSD: 3.444; p = 0.010) at the high topography than at

271 the low topography in the dry season (Table 1). In addition, Sal was significantly higher
272 in the dry season than in the rainy season, in both high (LSD: 2.916; $p < 0.001$) and low
273 (LSD: 3.003; $p < 0.001$) topographies (Table 1). (Table 1).

274 Table 1. Analysis of Sand (%), Silt (%), Clay (%), Moisture (%), pH, Redox Potential (Eh, mV) and salinity (Sal; ppt) in the mangrove soil of
 275 high and low topographies, and in the rainy and dry seasons (Macaca island, São Caetano das Odivelas). Numbers represent the mean \pm standard
 276 error of the mean. Lower case letters compare topographies in each seasonal period and upper-case letters compare the same topography between
 277 seasonal periods. Different letters indicate statistical difference (LSD, $p < 0.05$).

Season	Topography	Sand (%)	Silt (%)	Clay (%)	Moisture (%)	pH	Eh (mV)	Sal (ppt)
Dry	High	12.1 \pm 1.4 ^{aA}	41.8 \pm 3.3 ^{bA}	46.1 \pm 2.6 ^{aA}	73.1 \pm 6.6 ^{aA}	5.5 \pm 0.2 ^{aA}	190.25 \pm 45.53 ^{aA}	35.25 \pm 1.11 ^{aA}
	Low	9.7 \pm 2.5 ^{aA}	63.6 \pm 6.1 ^{aA}	26.6 \pm 5.2 ^{bA}	86.9 \pm 3.4 ^{aA}	5.3 \pm 0.3 ^{aA}	106.38 \pm 53.76 ^{aA}	30.13 \pm 1.16 ^{bA}
	Mean	10.9 \pm 1.4 ^A	52.7 \pm 4.4 ^A	36.4 \pm 3.8 ^A	80.0 \pm 4.0 ^A	5.4 \pm 0.2 ^A	148.31 \pm 35.71 ^A	32.69 \pm 1.02 ^A
Rainy	High	12.1 \pm 1.4 ^{aA}	41.8 \pm 3.3 ^{bA}	46.1 \pm 2.6 ^{aA}	88.9 \pm 3.5 ^{aA}	4.9 \pm 0.4 ^{aA}	92.50 \pm 56.20 ^{aA}	7.50 \pm 0.78 ^{aB}
	Low	9.7 \pm 2.5 ^{aA}	63.6 \pm 6.1 ^{aA}	26.6 \pm 5.2 ^{bA}	88.6 \pm 3.7 ^{aA}	4.4 \pm 0.1 ^{aB}	36.25 \pm 49.97 ^{aA}	8.13 \pm 0.79 ^{aB}
	Mean	10.9 \pm 1.4 ^A	52.7 \pm 4.4 ^A	36.4 \pm 3.8 ^A	88.7 \pm 2.5 ^A	4.6 \pm 0.2 ^B	64.38 \pm 37.04 ^A	7.81 \pm 0.54 ^B

278

279 The C_{mic} did not differ between topographies in the two seasons (Table 2). However, T_C
280 was significantly higher in the low topography in the dry season (LSD: 5.589; $p <$
281 0.000) and in the rainy season (LSD: 5.777; $p = 0.024$). In addition, C_{mic} was higher in
282 the dry season in both the high (LSD: 11.325; $p < 0.010$) and low (LSD: 9.345; $p <$
283 0.000) topographies (Table 2). N_{mic} did not vary between topographies seasonally.
284 However, N_{mic} in the high (LSD: 9.059; $p = 0.013$) and low topographies (LSD: 4.447;
285 $p = 0.001$) was higher during the dry season (Table 2). The C/N ratio (Table 2) was
286 higher in the low than in the high topography in both the dry (LSD: 3.142; $p < 0.000$)
287 and rainy seasons (LSD: 3.675; $p = 0.033$). However, only in the low topography was
288 the C/N ratio higher (LSD: 1.863; $p < 0.000$) in the dry season than in the rainy season
289 (Table 2). Soil OM was higher at the low topography in the rainy (LSD: 9.950; $p =$
290 0.024) and in the dry seasons (LSD: 9.630; $p < 0.000$). However, only in the lowland
291 topography was the OM concentration higher in the dry season than in the rainy season
292 (Table 2).

293 Table 2. Seasonal and topographic variation in microbial Carbon (C_{mic} ; $mg\ kg^{-1}$), microbial Nitrogen (N_{mic} , $mg\ kg^{-1}$), Total Carbon (T_C ; $g\ kg^{-1}$),
 294 Total Nitrogen (N_T ; $g\ kg^{-1}$), Carbon/Nitrogen ratio (C/N) and Soil Organic Matter (OM; $g\ kg^{-1}$). Numbers represent the mean (\pm standard error).
 295 Lower case letters compare topographies at each season, and upper-case letters compare the topography between seasons.

Season	Topography	C_{mic} $mg\ kg^{-1}$	N_{mic} $mg\ kg^{-1}$	T_C $g\ kg^{-1}$	T_N $g\ kg^{-1}$	C/N	OM $g\ kg^{-1}$
Dry	High	22.12 \pm 5.22 ^{aA}	12.76 \pm 4.20 ^{aA}	14.12 \pm 2.23 ^{bA}	1.43 \pm 0.06 ^{aA}	9.60 \pm 1.20 ^{bA}	24.35 \pm 3.84 ^{bA}
	Low	26.34 \pm 4.23 ^{aA}	10.34 \pm 2.05 ^{aA}	26.44 \pm 1.35 ^{aA}	1.56 \pm 0.04 ^{aA}	16.98 \pm 0.84 ^{aA}	45.59 \pm 2.32 ^{aA}
	Mean	24.23 \pm 3.29 ^A	11.55 \pm 2.28 ^A	20.28 \pm 2.03 ^A	1.49 \pm 0.04 ^A	13.29 \pm 1.19 ^A	34.97 \pm 3.50 ^A
Rainy	High	7.40 \pm 0.79 ^{aB}	0.75 \pm 0.41 ^{aB}	11.46 \pm 2.48 ^{bA}	1.32 \pm 0.04 ^{aA}	8.42 \pm 1.70 ^{bA}	19.75 \pm 4.27 ^{bA}
	Low	5.95 \pm 1.06 ^{aB}	1.23 \pm 0.28 ^{aB}	18.27 \pm 1.06 ^{aB}	1.46 \pm 0.06 ^{aA}	12.47 \pm 0.22 ^{aB}	31.51 \pm 1.83 ^{aB}
	Mean	6.68 \pm 0.67 ^B	0.99 \pm 0.25 ^B	14.86 \pm 1.57 ^B	1.39 \pm 0.04 ^A	10.44 \pm 0.98 ^A	25.63 \pm 2.71 ^B

296

297 **3.4 Vegetation structure and biomass**

298 Only the species *R. mangle* and *A. germinans* were found in the floristic survey carried
299 out. The DBH did not vary significantly between the topographies for either species
300 (Table 3). However, *R. mangle* had a higher DBH than *A. germinaris* at both high
301 (LSD: 139.304; $p = 0.037$) and low topographies (LSD: 131.307; $p = 0.001$). The basal
302 area (BA) and AGB did not show significant variation (Table 3). A total aboveground
303 biomass of $322.1 \pm 49.6 \text{ Mg ha}^{-1}$ was estimated.

304

305 Table 3: Summed Diameter at Breast Height (DBH; cm), Basal Area (BA; m² ha⁻¹) and Aboveground Biomass (AGB; Mg ha⁻¹) at high and low
 306 topographies in the mangrove forest of the Mojuim River estuary. Numbers represent the mean ± standard error of the mean. Lower case letters
 307 compare topographic height for each species, and upper-case letters compare species at each topographic height, using Tukey's test (p < 0.05).

Specie	Topography	N ha ⁻¹	DBH (cm)	BA (m ² ha ⁻¹)	AGB (Mg ha ⁻¹)
<i>Rhizophora mangle</i>	High	302.4±20.5	238.8±24.9 ^{aA}	17.3±2.0 ^{aA}	219.3±25.7 ^{aA}
	Low	310.4±37.6	283.5±45.0 ^{aA}	24.2±4.3 ^{aA}	338.7±62.9 ^{aA}
<i>Avicennia germinans</i>	High	47.7±20.5	86.8±51.2 ^{aB}	13.8±9.2 ^{aA}	135.3±94.7 ^{aA}
	Low	15.9±9.2	46.1±29.3 ^{aB}	11.8±8.8 ^{aA}	136.0±108.3 ^{aA}
Total	High	350.2±18.4	325.6±33.6 ^a	31.1±7.5 ^a	304.5±99.8 ^a
	Low	346.2±41.0	296.0±23.7 ^a	30.0±4.1 ^a	330.8±60.4 ^a

308 The equations for biomass estimates (AGB) were: *R. mangle* = 0.1282*DBH^{2.6}; *A. germinans* = 0.14*DBH^{2.4}; and Total = 0.168*ρ*DBH^{2.47}, where ρ_{*R. mangle*} = 0.87; ρ_{*A. germinans*}
 309 = 0.72 (Howard et al., 2014).

310

311 **3.5 Drivers of greenhouse gas fluxes**

312 In the rainy season, CO₂ efflux was correlated with T_{air} (Pearson = 0.23, p = 0.03), RH
313 (Pearson = -0.32, p < 0.00) and T_s (Pearson = 0.21, p = 0.04) only at the low
314 topography. In the dry season CO₂ flux was correlated with T_s (Pearson = 0.39, p <
315 0.00) at the low topography. The dry season was the period in which we found the
316 greatest amount of significant correlations between CO₂ efflux and soil chemical
317 parameters, while the C:N ratio, OM, and Eh were correlated with CO₂ efflux in both
318 seasons (Table 4). The negative correlation between T_C, N_T, C/N, and OM, along with
319 the positive correlation of N_{mic} with soil CO₂ flux, in the dry period, indicates that
320 microbial activity is a decisive factor for CO₂ efflux (Table 4). Soil moisture in the
321 Mojuim River mangrove forest negatively influenced CO₂ flux in both seasons (Table
322 4). However, soil moisture was not correlated with CH₄ flux. No significant correlations
323 were found between CH₄ efflux and the chemical properties of the soil in the mangrove
324 of the Mojuim River estuary (Table 4). However, more detailed studies on CH₄ efflux
325 and on its relationship with methanotrophic bacteria and abiotic factors (mainly
326 ammonia and sulfate) are needed due to the average flux of 4.70 mg C m⁻² h⁻¹ and the
327 extreme monthly and seasonal variations.

328

329 Table 4. Correlation coefficient (Pearson) of CO₂ and CH₄ fluxes with chemical parameters of the soil in a mangrove area in the Mojuim River
 330 estuary.

Gas Flux (g m ⁻² d ⁻¹)	Season	T _C (g kg ⁻¹)	T _N (g kg ⁻¹)	C _{mic} (mg kg ⁻¹)	N _{mic} (mg kg ⁻¹)	C/N	OM (g kg ⁻¹)	Sal (ppt)	Eh (mV)	pH	Moisture (%)
CO ₂	Dry	-0.68 ^{**}	-0.59 [*]	0.18 ^{NS}	0.61 ^{**}	-0.66 ^{**}	-0.67 ^{**}	-0.07 ^{NS}	0.51 [*]	0.21 ^{NS}	-0.49 [*]
	Rainy	-0.44 ^{NS}	-0.20 ^{NS}	-0.15 ^{NS}	-0.32 ^{NS}	-0.50 [*]	-0.63 ^{**}	-0.54 [*]	0.53 [*]	0.47 ^{NS}	-0.54 [*]
	Annual	-0.50 ^{**}	-0.35 [*]	-0.18 ^{NS}	0.00 ^{NS}	-0.53 ^{**}	-0.48 ^{**}	-0.30 ^{NS}	0.39 [*]	0.23 ^{NS}	-0.56 ^{**}
CH ₄	Dry	0.30 ^{NS}	0.07 ^{NS}	-0.14 ^{NS}	-0.24 ^{NS}	0.34 ^{NS}	0.02 ^{NS}	-0.04 ^{NS}	-0.38 ^{NS}	0.26 ^{NS}	0.26 ^{NS}
	Rainy	0.05 ^{NS}	-0.09 ^{NS}	0.44 ^{NS}	-0.27 ^{NS}	0.09 ^{NS}	-0.11 ^{NS}	-0.04 ^{NS}	-0.13 ^{NS}	-0.07 ^{NS}	0.04 ^{NS}
	Annual	0.04 ^{NS}	-0.10 ^{NS}	-0.01 ^{NS}	-0.18 ^{NS}	0.08 ^{NS}	-0.01 ^{NS}	-0.17 ^{NS}	-0.21 ^{NS}	-0.08 ^{NS}	0.02 ^{NS}

331 Total Carbon (T_C; g kg⁻¹); Total Nitrogen (T_N; g kg⁻¹); Microbial Carbon (C_{mic}, g kg⁻¹); Microbial Nitrogen (N_{mic}, g kg⁻¹); Carbon and Nitrogen
 332 ratio (C/N); Organic Matter (OM; g kg⁻¹); Salinity (Sal; ppt); Redox Potential (Eh; mV); Soil Moisture (Moisture, %).

333 NS= not significant; * significant effects at p ≤ 0.05; ** significant effects at p ≤ 0.01

334

335 4 Discussion

336 4.1 Carbon dioxide and methane flux

337 It is important to consider that the year under study was rainier in the dry season (2017)
338 and less rainy in the wet season (2018) when the climatological average is concerned
339 (1981-2010) (Figure 3). Perhaps this variation is related to the effects of global climate
340 changes. Under these conditions, negative and positive flows of the two greenhouse
341 gases were found (negative values represent gas consumption) Under these conditions,
342 the CO₂ flux from the mangrove soil ranged from -5.06 to 68.96 g CO₂ m⁻² d⁻¹ (mean
343 6.66 g CO₂ m⁻² d⁻¹), while the CH₄ flux ranged from -5.07 to 11.08 g CH₄ m⁻² d⁻¹ (mean
344 0.13 g CH₄ m⁻² d⁻¹), resulting in a total carbon rate of 1.92 g C m⁻² d⁻¹ or 7.00 Mg C ha⁻¹
345 y⁻¹ (Figure 2). The negative CO₂ flux is apparently a consequence of the increased CO₂
346 solubility in tidal waters or of the increased sulfate reduction, as described in the
347 literature (Borges et al., 2018; Chowdhury et al., 2018; Nóbrega et al., 2016).
348 Fluctuations in redox potential altered the availability of the terminal electron acceptor
349 and donor, and the forces of recovery of their concentrations in the soil, such that a
350 disproportionate release of CO₂ can result from the alternative anaerobic degradation
351 processes such as sulfate and iron reduction (Chowdhury et al., 2018). The soil carbon
352 flux in the mangrove area in the Amazon region was within the range of findings for
353 other tropical mangrove areas (2.57 to 11.00 g CO₂ m⁻² d⁻¹; Shiau and Chiu, 2020).
354 However, the mean flux of 6.2 mmol CO₂ m⁻² h⁻¹ recorded in this Amazonian mangrove
355 was much higher than the mean efflux of 2.9 mmol CO₂ m⁻² h⁻¹ recorded in 75
356 mangroves during low tide periods (Alongi, 2009).

357 An emission of 0.010 Tg CH₄ y⁻¹, 0.64 g CH₄ m⁻² d⁻¹ (Rosentreter et al., 2018a), or 26.7
358 mg CH₄ m⁻² h⁻¹ has been reported for tropical latitudes (0 and 5°). In our study, the
359 monthly average of CH₄ flux was higher at the low (7.3 ± 8.0 mg CH₄ m⁻² h⁻¹) than at
360 the high topography (0.9 ± 0.6 mg C m⁻² h⁻¹), resulting in 0.13 g CH₄ m⁻² d⁻¹ or 0.48 Mg
361 CH₄ ha⁻¹ y⁻¹ (Figure 2). Therefore, the CH₄-C fluxes from the mangrove soil in the
362 Mojuim River estuary were much lower than expected. It is known that there is a
363 microbial functional module for CH₄ production and consumption (Xu et al., 2015) and
364 diffusibility (Sihi et al., 2018), and considers three key mechanisms: aceticlastic
365 methanogenesis (acetate production), hydrogenotrophic methanogenesis (H₂ and CO₂
366 production), and aerobic methanotrophy (CH₄ oxidation and O₂ reduction). The average
367 emission from the soil of 8.4 mmol CH₄ m⁻² d⁻¹ was well below the fluxes recorded in

368 the Bay of Bengal, with $18.4 \text{ mmol CH}_4 \text{ m}^{-2} \text{ d}^{-1}$ (Biswas et al., 2007). In the Amazonian
369 mangrove studied the mean annual carbon equivalent efflux was $429.6 \text{ mg CO}_{2\text{-eq}} \text{ m}^{-2} \text{ h}^{-1}$.
370 ¹. This value is 0.00004% of the erosion losses of $103.5 \text{ Tg CO}_{2\text{-eq}} \text{ ha}^{-1} \text{ y}^{-1}$ projected for
371 the next century in tropical mangrove forests (Adame et al., 2021). These higher CO_2
372 flux concomitantly with lower CH_4 flux in this Amazonian estuary are probably a
373 consequence of changes in the rainfall pattern already underway, where the dry season
374 was wetter and the rainy season drier when compared to the climatological normal.

375 4.2 Drivers of greenhouse gas fluxes

376 Mangrove areas are periodically flooded, with a larger flood volume during the syzygy
377 tides, especially in the rainy season. The hydrological condition of the soil is determined
378 by the microtopography and can regulate the respiration of microorganisms (aerobic or
379 anaerobic), being a decisive factor in controlling the CO_2 efflux (Dai et al., 2012;
380 Davidson et al., 2000; Ehrenfeld, 1995). In the two climatic periods of the year, the high
381 topography produced more CO_2 ($7.869 \pm 1.873 \text{ g CO}_2 \text{ m}^{-2} \text{ d}^{-1}$) than the low topography
382 ($5.212 \pm 1.225 \text{ g CO}_2 \text{ m}^{-2} \text{ d}^{-1}$) (Figure 2; SI 1). No significant influence on CO_2 flux was
383 observed due to the low variation in high tide level throughout the year (0.19 m) (Figure
384 2), although it was numerically higher at the high topography. However, tidal height
385 and the rainy season resulted in a higher CO_2 flux (rate high/low =1.7) at the high
386 topography ($7.858 \pm 0.039 \text{ g CO}_2 \text{ m}^{-2} \text{ d}^{-1}$) than at the low topography ($4.734 \pm 0.335 \text{ g}$
387 $\text{CO}_2 \text{ m}^{-2} \text{ d}^{-1}$) (Figure 2; SI 1). This result is because the root systems of most flood-
388 tolerant plants remain active when flooded (Angelov et al., 1996). Still, the high
389 topography has longer flood-free periods, which only happens when the tides are
390 syzygy or when the rains are torrential.

391 CO_2 efflux was higher in the high topography than in the low topography in the rainy
392 season (when soils are more subject to inundation), i.e., 39.8% lower in the forest soil
393 exposed to the atmosphere for less time. Measurements performed on 62 mangrove
394 forest soils showed an average flux of $2.87 \text{ mmol CO}_2 \text{ m}^{-2} \text{ h}^{-1}$ when the soil was
395 exposed to the atmosphere, while 75 results on flooded mangrove forest soils showed an
396 average emission of $2.06 \text{ mmol CO}_2 \text{ m}^{-2} \text{ h}^{-1}$ (Alongi, 2007, 2009), i.e., 28.2% less than
397 for the dry soil. This reflects the increased facility gases have for molecular diffusion
398 than fluids, and the increased surface area available for aerobic respiration and chemical
399 oxidation during air exposure (Chen et al., 2010). Some studies attribute this variation
400 to the temperature of the soil when it is exposed to tropical air (Alongi, 2009), which

401 increases the export of dissolved inorganic carbon (Maher et al., 2018). However,
402 although despite the lack of significant variation in soil temperature between
403 topographies at each time of year (Figure 4b), there was a positive correlation (Pearson
404 = 0.15, $p = 0.05$) between CO₂ efflux and soil temperature at the low topography.

405 Some studies show that CH₄ efflux is a consequence of the seasonal temperature
406 variation in mangrove forest under temperate/monsoon climates (Chauhan et al., 2015;
407 Purvaja and Ramesh, 2001; Whalen, 2005). However, in your study CH₄ efflux was
408 correlated with Ta (Pearson = -0.33, $p < 0.00$) and RH (Pearson = 0.28, $p = 0.01$) only
409 in the dry season and at the low topography. The results show that the physical
410 parameters do not affect the fluxes in a standardized way, and their greater or lesser
411 influence depends on the topography and seasonality.

412 A compilation of several studies showed that the total CH₄ emissions from the soil in a
413 mangrove ecosystem range from 0 to 23.68 mg C m⁻² h⁻¹ (Shiau and Chiu, 2020), and
414 our study showed a range of -0.01 to 31.88 mg C m⁻² h⁻¹ (mean of 4.70 ± 5.00 mg C m⁻²
415 h⁻¹). The monthly CH₄ fluxes were generally higher at the low (0.232 ± 0.256) than at
416 the high (0.026 ± 0.018) topography, especially during the rainy season when the tides
417 were higher (Figure 2). Only in the dry season was there a significantly higher
418 production at the low than at the high topography (Figure 2; SI 1). The low topography
419 produced 0.0249 g C m⁻² h⁻¹ more to the atmosphere in the rainy season than in the dry
420 season (Figure 2), and a similar seasonal pattern was recorded in other studies
421 (Cameron et al., 2021).

422 The mangrove soil in the Mojuim River estuary is rich in silt and clay (Table 1), which
423 reduces sediment porosity and fosters the formation and maintenance of anoxic
424 conditions (Dutta et al., 2013). In addition, the lack of oxygen in the flooded mangrove
425 soil favors microbial processes such as denitrification, sulfate reduction,
426 methanogenesis, and redox reactions (Alongi and Christoffersen, 1992). A significant
427 amount of CH₄ produced in wetlands is dissolved in the pore water due to high pressure,
428 causing supersaturation, which allows CH₄ to be released by diffusion from the
429 sediment to the atmosphere and by boiling through the formation of bubbles.

430 Studies show that the CO₂ flux tends to be lower with high soil saturation (Chanda et
431 al., 2014; Kristensen et al., 2008). A total of 395 Mg C ha⁻¹ was found at the soil surface
432 (0.15 m) in the mangrove of the Mojuim River estuary, which was slightly higher than
433 the 340 Mg C ha⁻¹ found in other mangroves in the Amazon (Kauffman et al., 2018),

434 however being significantly 1.8 times greater at the low topography (Table 2). The finer
435 soil texture at the low topography (Table 1) reduces groundwater drainage which
436 facilitates the accumulation of C in the soil (Schmidt et al., 2011).

437 **4.3 Mangrove biomass**

438 Only the species *R. mangle* and *A. germinans* were found in the floristic survey carried
439 out, which is aligned with the results of other studies in the same region (Menezes et al.,
440 2008). Thus, the variations found in the flux between the topographies in the Mojuim
441 River estuary are not related to the mangrove forest structure, because there was no
442 difference in the aboveground biomass. Since there was no difference in the species
443 composition, the belowground biomass is not expected to differ either (Table 3).

444 Assuming that the amount of carbon stored is 0.42 of the total biomass (Sahu and
445 Kathiresan, 2019), the mangrove forest biomass of the Mojuim River estuary stores
446 127.9 and 138.9 Mg C ha⁻¹ at the high and low topographies, respectively. This result is
447 well below the 507.8 Mg C ha⁻¹ estimated for Brazilian mangroves (Hamilton and
448 Friess, 2018), but are near the 103.7 Mg C ha⁻¹ estimated for a mangrove at Guara's
449 island (Salum et al., 2020), 108.4 Mg C ha⁻¹ for the Bragantina region (Gardunho,
450 2017), and 132.3 Mg C ha⁻¹ in French Guiana (Fromard et al., 1998). The biomass
451 found in the Mojuim estuary does not differ from the biomass found in other
452 Amazonian mangroves, despite being much lower than that found in other Brazilian
453 mangroves. The estimated primary production for tropical mangrove forests is 218 ± 72
454 Tg C y (Bouillon et al., 2008).

455 **4.4 Biogeochemical parameters**

456 During the seasonal and annual periods, CH₄ efflux was not significantly correlated
457 with chemical parameters (Table 5), which is similar to the observed in another study
458 (Chen et al., 2010). Flooded soils present reduced gas diffusion rates, which directly
459 affects the physiological state and activity of microbes, by limiting the supply of the
460 dominant electron acceptors (e.g., oxygen), and gases (e.g., CH₄) (Blagodatsky and
461 Smith, 2012). The importance of soil moisture was evident in the richness and diversity
462 of bacterial communities in a study that compared the different pore spaces filled with
463 water (Banerjee et al., 2016). Furthermore, sulfate reduction in flooded soils (another
464 pathway of organic matter metabolism) is dependent on the redox potential of the soil.
465 However, no sulfate reduction occurs when the redox potential has values are above -

466 150 mv (Connell and Patrick, 1968). In our study, Eh was above 36.0 mV indicating
467 that sulfate reduction probably did not influence the OM metabolism.

468 On the other hand, increasing soil moisture provides the microorganisms with essential
469 substrates such as ammonium, nitrate, and soluble organic carbon, and increases gas
470 diffusion rates in the water (Blagodatsky and Smith, 2012). Biologically available
471 nitrogen often limit marine productivity (Bertics et al., 2010), and thus can affect CO₂
472 fluxes to the atmosphere. However, a mangrove fertilization experiment showed that
473 CH₄ emission rates were not affected by N addition (Kreuzwieser et al., 2003). A higher
474 concentration of C_{mic} and N_{mic} in the dry period (Table 2), both in the high and low
475 topographies, indicated that microorganisms are more active when the soil spends more
476 time aerated in the dry period (Table 2), period when only the high tides produce anoxia
477 in the mangrove soil mainly in the low topography. Under reduced oxygen conditions,
478 in a laboratory incubated mangrove soil, the addition of nitrogen resulted in a
479 significant increase in the microbial metabolic quotient, showing no concomitant
480 change in microbial respiration, which was explained by a decrease in microbial
481 biomass (Craig et al., 2021).

482 The high OM concentration at the two topographic heights (Table 2), at the two seasons
483 studied, and the respective negative correlation with CO₂ flux (Table 5) confirm the
484 importance of microbial activity in mangrove soils (Gao et al., 2020). Also, CH₄
485 produced in flooded soils can be converted mainly to CO₂ by the anaerobic oxidation of
486 CH₄ (Boetius et al., 2000; Milucka et al., 2015; Xu et al., 2015) which may contribute to
487 the higher CO₂ efflux in the Mojuim River estuary compared to other tropical
488 mangroves (Rosentreter et al., 2018b). The belowground C stock is considered the
489 largest C reservoir in a mangrove ecosystem, and it results from the low OM
490 decomposition rate due to flooding (Marchand, 2017).

491 The higher water salinity influenced by the tidal movement in the dry season (Table 1)
492 seems to result in a lower CH₄ flux at the low topography (Dutta et al., 2013; Lekphet et
493 al., 2005; Shiao and Chiu, 2020). Sulfate (SO₄²⁻) in the brine affects the competition
494 between SO₄²⁻ reduction and methanogenic fermentation, as sulfate-reducing bacteria
495 are more efficient at using hydrogen than methanotrophic bacteria (Abram and Nedwell,
496 1978; Kristjansson et al., 1982), a key factor fostering reduced CH₄ emissions. At high
497 SO₄²⁻ concentrations methanotrophic bacteria use CH₄ as an energy source and oxidize
498 it to CO₂ (Coyne, 1999; Segarra et al., 2015), increasing the efflux of CO₂ and reduced

499 CH₄ (Meronigal and Schlesinger, 2002; Roslev and King, 1996). This may explain the
500 high CO₂ efflux found throughout the year at the high and, especially, at the low
501 topographies (Figure 3).

502 Studies in coastal ecosystems in Taiwan have reported that methanotrophic bacteria can
503 be sensitive to soil pH, and reported an optimal growth at pH ranging from 6.5 to 7.5
504 (Shiau et al., 2018). The higher soil acidity in the Mojuim River wetland (Table 1) may
505 be inhibiting the activity of methanogenic bacteria by increasing the population of
506 methanotrophic bacteria, which are efficient in CH₄ consumption (Chen et al., 2010;
507 Hegde et al., 2003; Shiau and Chiu, 2020). In addition, the pneumatophores present in
508 *R. mangle* increase soil aeration and reduce CH₄ emissions (Allen et al., 2011; He et al.,
509 2019). Spatial differences (topography) in CH₄ emissions in the soil can be attributed to
510 substrate heterogeneity, salinity, and the abundance of methanogenic and
511 methanotrophic bacteria (Gao et al., 2020). The high Eh values found in both
512 topographies, mainly in the dry period (Table 1), hinder CH₄ emission. Soil Eh above -
513 150 mV has been considered limiting for CH₄ production (Yang and Chang, 1998).
514 Increases in CH₄ efflux with reduced salinity were found as a consequence of intense
515 oxidation or reduced competition from the more energetically efficient SO₄²⁻ and NO₃³⁻
516 reducing bacteria when compared to the methanogenic bacteria (Biswas et al., 2007).
517 This fact can be observed in the CH₄ efflux in the mangrove of the Mojuim River,
518 because there was an increased CH₄ production especially in the low topography in the
519 rainy season (Figure 3), when water salinity is reduced (Table 1) due to the increased
520 precipitation. However, we did not find a correlation between CH₄ efflux and salinity,
521 as previously reported (Purvaja and Ramesh, 2001)

522 5 Conclusions

523 The most recent estimate between latitude 0° to 23.5° S shows an emission of 2.3 g CO₂
524 m⁻² d⁻¹ (Rosentreter et al., 2018b). However, the efflux in the mangrove of the Mojuim
525 River estuary was 6.7 g CO₂ m⁻² d⁻¹. For the same latitudinal range, Rosentreter et al.
526 (2018c) estimated an emission of 0.64 g CH₄ m⁻² d⁻¹, and we found an efflux of 0.13 g
527 CH₄ m⁻² d⁻¹. Seasonality was important for CH₄ efflux but did not influence CO₂ efflux.
528 The differences in fluxes may be an effect of global climate changes on the terrestrial
529 biogeochemistry at the plant-soil-atmosphere interface, as indicated by the deviation in
530 precipitation values from the climatology normal, making it necessary to extend this
531 study for more years. Using the factor of 23 to convert the global warming potential of

532 CH₄ to CO₂ (IPCC, 2001), the CO₂ equivalent emission was 35.4 Mg CO_{2-eq} ha⁻¹ yr⁻¹.
533 Over a 100-year time period, a radiative forcing due to the continuous emission of 0.05
534 kg CH₄ m⁻² y⁻¹ found in this study, would be offset if CO₂ sequestration rates were 2.16
535 kg CO₂ m⁻² y⁻¹ (Neubauer and Megonigal, 2015).

536 Microtopography should be considered when determining the efflux of CO₂ and CH₄ in
537 mangrove forests in an Amazon estuary. The low topography in the mangrove forest of
538 Mojuim River had a higher concentration of organic carbon in the soil. However, it did
539 not produce a higher CO₂ efflux because it was negatively influenced by soil moisture,
540 which was indifferent to CH₄ efflux. MO, C/N ratio, and Eh were critical in soil
541 microbial activity, which resulted in a variation in CO₂ flux during the year and
542 seasonal periods. Thus, the physicochemical properties of the soil are important for CO₂
543 flux, especially in the rainy season. Still, they did not influence CH₄ fluxes.

544 **Data availability:** The data used in this article belong to the doctoral thesis of Saul
545 Castellón, within the Postgraduate Program in Environmental Sciences, at the Federal
546 University of Pará. Access to the data can be requested from Dr. Castellón
547 (saulmarz22@gmail.com), which holds the set of all data used in this paper.

548 **Author contributions:** SEMC and JHC designed the study and wrote the article with the
549 help of JFB, MR, MLR, and CN. JFB assisted in the field experiment. MR provided
550 logistical support in field activities.

551 **Competing interests:** The authors declare that they have no conflict of interest

552 **Acknowledgements:** The authors are grateful to the Program of Alliances for Education
553 and Training of the Organization of the American States and to Coimbra Group of
554 Brazilian Universities, for the financial support, as well as to Paulo Sarmiento for the
555 assistance at laboratory analysis, and to Maridalva Ribeiro and Lucivaldo da Silva for
556 the fieldwork assistance. Furthermore, the authors would like to thank the Laboratory of
557 Biogeochemical Cycles (Geosciences Institute, Federal University of Pará) for the
558 equipment provided for this research.

559 **6 References**

560 Abram, J. W. and Nedwell, D. B.: Inhibition of methanogenesis by sulphate reducing
561 bacteria competing for transferred hydrogen, Arch. Microbiol., 117(1), 89–92,
562 doi:10.1007/BF00689356, 1978.

563 Adame, M. F., Connolly, R. M., Turschwell, M. P., Lovelock, C. E., Fatoyinbo, T.,
564 Lagomasino, D., Goldberg, L. A., Holdorf, J., Friess, D. A., Sasmito, S. D., Sanderman,
565 J., Sievers, M., Buelow, C., Kauffman, J. B., Bryan-Brown, D. and Brown, C. J.: Future
566 carbon emissions from global mangrove forest loss, *Glob. Chang. Biol.*, 27(12), 2856–
567 2866, doi:10.1111/gcb.15571, 2021.

568 Allen, D., Dalal, R. C., Rennenberg, H. and Schmidt, S.: Seasonal variation in nitrous
569 oxide and methane emissions from subtropical estuary and coastal mangrove sediments,
570 Australia, *Plant Biol.*, 13(1), 126–133, doi:10.1111/j.1438-8677.2010.00331.x, 2011.

571 Almeida, R. F. de, Mikhael, J. E. R., Franco, F. O., Santana, L. M. F. and Wendling, B.:
572 Measuring the labile and recalcitrant pools of carbon and nitrogen in forested and
573 agricultural soils: A study under tropical conditions, *Forests*, 10(7), 544,
574 doi:10.3390/f10070544, 2019.

575 Alongi, D. M.: The contribution of mangrove ecosystems to global carbon cycling and
576 greenhouse gas emissions, in *Greenhouse gas and carbon balances in mangrove coastal*
577 *ecosystems*, edited by Y. Tateda, R. Upstill-Goddard, T. Goreau, D. M. Alongi, A.
578 Nose, E. Kristensen, and G. Wattayakorn, pp. 1–10, Gendai Tosho, Kanagawa, Japan.,
579 2007.

580 Alongi, D. M.: *The energetics of mangrove forests*, Springer., 2009.

581 Alongi, D. M. and Christoffersen, P.: Benthic infauna and organism-sediment relations
582 in a shallow, tropical coastal area: influence of outwelled mangrove detritus and
583 physical disturbance, *Mar. Ecol. Prog. Ser.*, 81(3), 229–245, doi:10.3354/meps081229,
584 1992.

585 Alongi, D. M. and Mukhopadhyay, S. K.: Contribution of mangroves to coastal carbon
586 cycling in low latitude seas, *Agric. For. Meteorol.*, 213, 266–272,
587 doi:10.1016/j.agrformet.2014.10.005, 2015.

588 Angelov, M. N., Sung, S. J. S., Doong, R. Lou, Harms, W. R., Kormanik, P. P. and
589 Black, C. C.: Long-and short-term flooding effects on survival and sink-source
590 relationships of swamp-adapted tree species, *Tree Physiol.*, 16(4), 477–484,
591 doi:10.1093/treephys/16.5.477, 1996.

592 Araujo, A. S. F. de: Is the microwave irradiation a suitable method for measuring soil
593 microbial biomass?, *Rev. Environ. Sci. Biotechnol.*, 9(4), 317–321,

594 doi:10.1007/s11157-010-9210-y, 2010.

595 Banerjee, S., Helgason, B., Wang, L., Winsley, T., Ferrari, B. C. and Siciliano, S. D.:
596 Legacy effects of soil moisture on microbial community structure and N₂O emissions,
597 *Soil Biol. Biochem.*, 95, 40–50, doi:10.1016/j.soilbio.2015.12.004, 2016.

598 Bastviken, D., Tranvik, L. J., Downing, J. A., Crill, P. M. and Enrich-Prast, A.:
599 Freshwater Methane Emissions Offset the Continental Carbon Sink, *Science* (80-.),
600 331(6013), 50–50, doi:10.1126/science.1196808, 2011.

601 Bauza, J. F., Morell, J. M. and Corredor, J. E.: Biogeochemistry of Nitrous Oxide
602 Production in the Red Mangrove (*Rhizophora mangle*) Forest Sediments, *Estuar. Coast.*
603 *Shelf Sci.*, 55(5), 697–704, doi:10.1006/ECSS.2001.0913, 2002.

604 Bertics, V. J., Sohm, J. A., Treude, T., Chow, C. E. T., Capone, D. G., Fuhrman, J. A.
605 and Ziebis, W.: Burrowing deeper into benthic nitrogen cycling: The impact of
606 Bioturbation on nitrogen fixation coupled to sulfate reduction, *Mar. Ecol. Prog. Ser.*,
607 409, 1–15, doi:10.3354/meps08639, 2010.

608 Biswas, H., Mukhopadhyay, S. K., Sen, S. and Jana, T. K.: Spatial and temporal
609 patterns of methane dynamics in the tropical mangrove dominated estuary, NE coast of
610 Bay of Bengal, India, *J. Mar. Syst.*, 68(1–2), 55–64, doi:10.1016/j.jmarsys.2006.11.001,
611 2007.

612 Blagodatsky, S. and Smith, P.: Soil physics meets soil biology: Towards better
613 mechanistic prediction of greenhouse gas emissions from soil, *Soil Biol. Biochem.*, 47,
614 78–92, doi:10.1016/J.SOILBIO.2011.12.015, 2012.

615 Boetius, A., Ravenschlag, K., Schubert, C. J., Rickert, D., Widdel, F., Gleseke, A.,
616 Amann, R., Jørgensen, B. B., Witte, U. and Pfannkuche, O.: A marine microbial
617 consortium apparently mediating anaerobic oxidation methane, *Nature*, 407(6804), 623–
618 626, doi:10.1038/35036572, 2000.

619 Borges, A. V., Abril, G., Darchambeau, F., Teodoru, C. R., Deborde, J., Vidal, L. O.,
620 Lambert, T. and Bouillon, S.: Divergent biophysical controls of aquatic CO₂ and CH₄
621 in the World’s two largest rivers, *Sci. Rep.*, 5, doi:10.1038/srep15614, 2015.

622 Borges, A. V., Abril, G. and Bouillon, S.: Carbon dynamics and CO₂ and CH₄
623 outgassing in the Mekong delta, *Biogeosciences*, 15(4), doi:10.5194/bg-15-1093-2018,
624 2018.

625 Bouillon, S., Borges, A. V., Castañeda-Moya, E., Diele, K., Dittmar, T., Duke, N. C.,
626 Kristensen, E., Lee, S. Y., Marchand, C., Middelburg, J. J., Rivera-Monroy, V. H.,
627 Smith, T. J. and Twilley, R. R.: Mangrove production and carbon sinks: A revision of
628 global budget estimates, *Global Biogeochem. Cycles*, 22(2),
629 doi:10.1029/2007GB003052, 2008.

630 Brookes, P. C., Landman, A., Pruden, G. and Jenkinson, D. S.: Chloroform fumigation
631 and the release of soil nitrogen: A rapid direct extraction method to measure microbial
632 biomass nitrogen in soil, *Soil Biol. Biochem.*, 17(6), 837–842, doi:10.1016/0038-
633 0717(85)90144-0, 1985.

634 Cameron, C., Hutley, L. B., Munksgaard, N. C., Phan, S., Aung, T., Thinn, T., Aye, W.
635 M. and Lovelock, C. E.: Impact of an extreme monsoon on CO₂ and CH₄ fluxes from
636 mangrove soils of the Ayeyarwady Delta, Myanmar, *Sci. Total Environ.*, 760, 143422,
637 doi:10.1016/j.scitotenv.2020.143422, 2021.

638 Castillo, J. A. A., Apan, A. A., Maraseni, T. N. and Salmo, S. G.: Soil greenhouse gas
639 fluxes in tropical mangrove forests and in land uses on deforested mangrove lands,
640 *Catena*, 159, 60–69, doi:10.1016/j.catena.2017.08.005, 2017.

641 Chanda, A., Akhand, A., Manna, S., Dutta, S., Das, I., Hazra, S., Rao, K. H. and
642 Dadhwal, V. K.: Measuring daytime CO₂ fluxes from the inter-tidal mangrove soils of
643 Indian Sundarbans, *Environ. Earth Sci.*, 72(2), 417–427, doi:10.1007/s12665-013-2962-
644 2, 2014.

645 Chauhan, R., Datta, A., Ramanathan, A. and Adhya, T. K.: Factors influencing spatio-
646 temporal variation of methane and nitrous oxide emission from a tropical mangrove of
647 eastern coast of India, *Atmos. Environ.*, 107, 95–106,
648 doi:10.1016/j.atmosenv.2015.02.006, 2015.

649 Chen, G. C., Tam, N. F. Y. and Ye, Y.: Spatial and seasonal variations of atmospheric
650 N₂O and CO₂ fluxes from a subtropical mangrove swamp and their relationships with
651 soil characteristics, *Soil Biol. Biochem.*, 48, 175–181,
652 doi:10.1016/j.soilbio.2012.01.029, 2012.

653 Chen, G. C., Ulumuddin, Y. I., Pramudji, S., Chen, S. Y., Chen, B., Ye, Y., Ou, D. Y.,
654 Ma, Z. Y., Huang, H. and Wang, J. K.: Rich soil carbon and nitrogen but low
655 atmospheric greenhouse gas fluxes from North Sulawesi mangrove swamps in
656 Indonesia, *Sci. Total Environ.*, 487(1), 91–96, doi:10.1016/j.scitotenv.2014.03.140,

657 2014.

658 Chen, G. C. C., Tam, N. F. Y. F. Y. and Ye, Y.: Summer fluxes of atmospheric
659 greenhouse gases N₂O, CH₄ and CO₂ from mangrove soil in South China, *Sci. Total*
660 *Environ.*, 408(13), 2761–2767, doi:10.1016/j.scitotenv.2010.03.007, 2010.

661 Chowdhury, T. R., Bramer, L., Hoyt, D. W., Kim, Y. M., Metz, T. O., McCue, L. A.,
662 Diefenderfer, H. L., Jansson, J. K. and Bailey, V.: Temporal dynamics of CO₂ and CH₄
663 loss potentials in response to rapid hydrological shifts in tidal freshwater wetland soils,
664 *Ecol. Eng.*, 114, 104–114, doi:10.1016/j.ecoleng.2017.06.041, 2018.

665 Chuang, P. C., Young, M. B., Dale, A. W., Miller, L. G., Herrera-Silveira, J. A. and
666 Paytan, A.: Methane and sulfate dynamics in sediments from mangrove-dominated
667 tropical coastal lagoons, Yucatan, Mexico, *Biogeosciences*, 13(10), 2981–3001, 2016.

668 Connell, W. E. and Patrick, W. H.: Sulfate Reduction in Soil: Effects of Redox Potential
669 and p H, *Science* (80-.), 159(3810), 86–87, doi:10.1126/science.159.3810.86, 1968.

670 Coyne, M.: *Soil Microbiology: An Exploratory Approach*, Delmar Publishers, New
671 York, NY, USA., 1999.

672 Craig, H., Antwis, R. E., Cordero, I., Ashworth, D., Robinson, C. H., Osborne, T. Z.,
673 Bardgett, R. D., Rowntree, J. K. and Simpson, L. T.: Nitrogen addition alters
674 composition, diversity, and functioning of microbial communities in mangrove soils:
675 An incubation experiment, *Soil Biol. Biochem.*, 153, 108076,
676 doi:10.1016/j.soilbio.2020.108076, 2021.

677 Dai, Z., Trettin, C. C., Li, C., Li, H., Sun, G. and Amatya, D. M.: Effect of Assessment
678 Scale on Spatial and Temporal Variations in CH₄, CO₂, and N₂O Fluxes in a Forested
679 Wetland, *Water, Air, Soil Pollut.*, 223(1), 253–265, doi:10.1007/s11270-011-0855-0,
680 2012.

681 Davidson, E. A., Verchot, L. V., Cattanio, J. H., Ackerman, I. L. and Carvalho, J. E. M.:
682 Effects of soil water content on soil respiration in forests and cattle pastures of eastern
683 Amazonia, *Biogeochemistry*, 48(1), 53–69, doi:10.1023/a:1006204113917, 2000.

684 Donato, D. C., Kauffman, J. B., Murdiyarso, D., Kurnianto, S., Stidham, M. and
685 Kanninen, M.: Mangroves among the most carbon-rich forests in the tropics, *Nat.*
686 *Geosci.*, 4(5), 293–297, doi:10.1038/ngeo1123, 2011.

687 Dutta, M. K., Chowdhury, C., Jana, T. K. and Mukhopadhyay, S. K.: Dynamics and

688 exchange fluxes of methane in the estuarine mangrove environment of the Sundarbans,
689 NE coast of India, *Atmos. Environ.*, 77, 631–639, doi:10.1016/j.atmosenv.2013.05.050,
690 2013.

691 Ehrenfeld, J. G.: Microsite differences in surface substrate characteristics in
692 *Chamaecyparis* swamps of the New Jersey Pinelands, *Wetlands*, 15(2), 183–189,
693 doi:10.1007/BF03160672, 1995.

694 El-Robrini, M., Alves, M. A. M. S., Souza Filho, P. W. M., El-Robrini M. H. S., Silva
695 Júnior, O. G. and França, C. F.: Atlas de Erosão e Progradação da zona costeira do
696 Estado do Pará – Região Amazônica: Áreas oceânica e estuarina, in Atlas de Erosão e
697 Progradação da Zona Costeira Brasileira, edited by D. Muehe, pp. 1–34, São Paulo.,
698 2006.

699 EPA, E. P. A.: Inventory of U.S. Greenhouse Gas Emissions and Sinks: 1990–2015.,
700 2017.

701 Fernandes, W. A. A. and Pimentel, M. A. da S.: Dinâmica da paisagem no entorno da
702 RESEX marinha de São João da Ponta/PA: utilização de métricas e geoprocessamento,
703 *Caminhos Geogr.*, 20(72), 326–344, doi:10.14393/RCG207247140, 2019.

704 Ferreira, A. S., Camargo, F. A. O. and Vidor, C.: Utilização de microondas na avaliação
705 da biomassa microbiana do solo, *Rev. Bras. Ciência do Solo*, 23(4), 991–996,
706 doi:10.1590/S0100-06831999000400026, 1999.

707 Ferreira, S. da S.: Entre marés e mangues: paisagens territorializadas por pescadores da
708 resex marinha de São João da Ponta/PA /, Universidade Federal do Pará., 2017.

709 França, C. F. de, Pimentel, M. A. D. S. and Neves, S. C. R.: Estrutura Paisagística De
710 São João Da Ponta, Nordeste Do Pará, *Geogr. Ensino Pesqui.*, 20(1), 130–142,
711 doi:10.5902/2236499418331, 2016.

712 Frankignoulle, M.: Field measurements of air-sea CO₂ exchange, *Limnol. Oceanogr.*,
713 33(3), 313–322, 1988.

714 Friesen, S. D., Dunn, C. and Freeman, C.: Decomposition as a regulator of carbon
715 accretion in mangroves: a review, *Ecol. Eng.*, 114, 173–178,
716 doi:10.1016/j.ecoleng.2017.06.069, 2018.

717 Fromard, F., Puig, H., Cadamuro, L., Marty, G., Betoulle, J. L. and Mougin, E.:
718 Structure, above-ground biomass and dynamics of mangrove ecosystems: new data

719 from French Guiana, *Oecologia*, 115(1), 39–53, doi:10.1007/s004420050489, 1998.

720 Gao, G. F., Zhang, X. M., Li, P. F., Simon, M., Shen, Z. J., Chen, J., Gao, C. H. and
721 Zheng, H. L.: Examining Soil Carbon Gas (CO₂, CH₄) Emissions and the Effect on
722 Functional Microbial Abundances in the Zhangjiang Estuary Mangrove Reserve, *J.*
723 *Coast. Res.*, 36(1), 54–62, doi:10.2112/JCOASTRES-D-18-00107.1, 2020.

724 Gardunho, D. C. L.: Estimativas de biomassa acima do solo da floresta de mangue na
725 península de Ajuruteua, Bragança – PA, Federal University of Pará, Belém, Brazil.,
726 2017.

727 Hamilton, S. E. and Friess, D. A.: Global carbon stocks and potential emissions due to
728 mangrove deforestation from 2000 to 2012, *Nat. Clim. Chang.*, 8(3), 240–244,
729 doi:10.1038/s41558-018-0090-4, 2018.

730 He, Y., Guan, W., Xue, D., Liu, L., Peng, C., Liao, B., Hu, J., Zhu, Q., Yang, Y., Wang,
731 X., Zhou, G., Wu, Z. and Chen, H.: Comparison of methane emissions among invasive
732 and native mangrove species in Dongzhaigang, Hainan Island, *Sci. Total Environ.*, 697,
733 133945, doi:10.1016/j.scitotenv.2019.133945, 2019.

734 Hegde, U., Chang, T.-C. and Yang, S.-S.: Methane and carbon dioxide emissions from
735 Shan-Chu-Ku landfill site in northern Taiwan., *Chemosphere*, 52(8), 1275–1285,
736 doi:10.1016/S0045-6535(03)00352-7, 2003.

737 Herz, R.: *Manguezais do Brasil*, Instituto Oceanografico da Usp/Cirm, São Paulo,
738 Brazil., 1991.

739 Howard, J., Hoyt, S., Isensee, K., Telszewski, M. and Pidgeon, E.: Coastal Blue
740 Carbon: Methods for Assessing Carbon Stocks and Emissions Factors in Mangroves,
741 Tidal Salt Marshes, and Seagrasses, edited by J. Howard, S. Hoyt, K. Isensee, M.
742 Telszewski, and E. Pidgeon, International Union for Conservation of Nature, Arlington,
743 Virginia, USA. [online] Available from: [http://www.unesco.org/new/en/natural-](http://www.unesco.org/new/en/natural-sciences/ioc-oceans/sections-and-programmes/ocean-sciences/ocean-carbon/coastal-blue-carbon/)
744 [sciences/ioc-oceans/sections-and-programmes/ocean-sciences/ocean-carbon/coastal-](http://www.unesco.org/new/en/natural-sciences/ioc-oceans/sections-and-programmes/ocean-sciences/ocean-carbon/coastal-blue-carbon/)
745 [blue-carbon/](http://www.unesco.org/new/en/natural-sciences/ioc-oceans/sections-and-programmes/ocean-sciences/ocean-carbon/coastal-blue-carbon/) (Accessed 11 September 2019), 2014.

746 IPCC: *Climate Change 2001: Third Assessment Report of the IPCC*, Cambridge., 2001.

747 Islam, K. R. and Weil, R. R.: Microwave irradiation of soil for routine measurement of
748 microbial biomass carbon, *Biol. Fertil. Soils*, 27(4), 408–416,
749 doi:10.1007/s003740050451, 1998.

750 Kalembasa, S. J. and Jenkinson, D. S.: A comparative study of titrimetric and
751 gravimetric methods for determination of organic carbon in soil, *J. Sci. Food Agric.*, 24,
752 1085–1090, 1973.

753 Kauffman, B. J., Donato, D. and Adame, M. F.: Protocolo para la medición, monitoreo
754 y reporte de la estructura, biomasa y reservas de carbono de los manglares, Bogor,
755 Indonesia., 2013.

756 Kauffman, J. B., Bernardino, A. F., Ferreira, T. O., Giovannoni, L. R., De Gomes, L. E.
757 O., Romero, D. J., Jimenez, L. C. Z. and Ruiz, F.: Carbon stocks of mangroves and salt
758 marshes of the Amazon region, Brazil, *Biol. Lett.*, 14(9), doi:10.1098/rsbl.2018.0208,
759 2018.

760 Kreuzwieser, J., Buchholz, J. and Rennenberg, H.: Emission of Methane and Nitrous
761 Oxide by Australian Mangrove Ecosystems, *Plant Biol.*, 5(4), 423–431, doi:10.1055/s-
762 2003-42712, 2003.

763 Kristensen, E., Bouillon, S., Dittmar, T. and Marchand, C.: Organic carbon dynamics in
764 mangrove ecosystems: A review, *Aquat. Bot.*, 89(2), 201–219,
765 doi:10.1016/J.AQUABOT.2007.12.005, 2008.

766 Kristjansson, J. K., Schönheit, P. and Thauer, R. K.: Different K_s values for hydrogen
767 of methanogenic bacteria and sulfate reducing bacteria: An explanation for the apparent
768 inhibition of methanogenesis by sulfate, *Arch. Microbiol.*, 131(3), 278–282,
769 doi:10.1007/BF00405893, 1982.

770 Lekphet, S., Nitorisavut, S. and Adsavakulchai, S.: Estimating methane emissions from
771 mangrove area in Ranong Province, Thailand, *Songklanakarin J. Sci. Technol.* , 27(1),
772 153–163 [online] Available from: <https://www.researchgate.net/publication/26473398>
773 (Accessed 29 January 2019), 2005.

774 Maher, D. T., Call, M., Santos, I. R. and Sanders, C. J.: Beyond burial: Lateral
775 exchange is a significant atmospheric carbon sink in mangrove forests, *Biol. Lett.*,
776 14(7), 1–4, doi:10.1098/rsbl.2018.0200, 2018.

777 Mahesh, P., Sreenivas, G., Rao, P. V. N. N., Dadhwal, V. K., Sai Krishna, S. V. S. S.
778 and Mallikarjun, K.: High-precision surface-level CO₂ and CH₄ using off-axis
779 integrated cavity output spectroscopy (OA-ICOS) over Shadnagar, India, *Int. J. Remote*
780 *Sens.*, 36(22), 5754–5765, doi:10.1080/01431161.2015.1104744, 2015.

781 Marchand, C.: Soil carbon stocks and burial rates along a mangrove forest
782 chronosequence (French Guiana), *For. Ecol. Manage.*, 384, 92–99,
783 doi:10.1016/j.foreco.2016.10.030, 2017.

784 McEwing, K. R., Fisher, J. P. and Zona, D.: Environmental and vegetation controls on
785 the spatial variability of CH₄ emission from wet-sedge and tussock tundra ecosystems
786 in the Arctic, *Plant Soil*, 388(1–2), 37–52, doi:10.1007/s11104-014-2377-1, 2015.

787 Megonigal, J. P. and Schlesinger, W. H.: Methane-limited methanotrophy in tidal
788 freshwater swamps, *Global Biogeochem. Cycles*, 16(4), 35-1-35–10,
789 doi:10.1029/2001GB001594, 2002.

790 Menezes, M. P. M. de, Berger, U. and Mehlig, U.: Mangrove vegetation in Amazonia :
791 a review of studies from the coast of Pará and Maranhão States , north Brazil, *Acta*
792 *Amaz.*, 38(3), 403–420, doi:10.1590/S0044-59672008000300004, 2008.

793 Milucka, J., Kirf, M., Lu, L., Krupke, A., Lam, P., Littmann, S., Kuypers, M. M. M. and
794 Schubert, C. J.: Methane oxidation coupled to oxygenic photosynthesis in anoxic
795 waters, *ISME J.*, 9(9), 1991–2002, doi:10.1038/ismej.2015.12, 2015.

796 Monz, C. A., Reuss, D. E. and Elliott, E. T.: Soil microbial biomass carbon and nitrogen
797 estimates using 2450 MHz microwave irradiation or chloroform fumigation followed by
798 direct extraction, *Agric. Ecosyst. Environ.*, 34(1–4), 55–63, doi:10.1016/0167-
799 8809(91)90093-D, 1991.

800 Neubauer, S. C. and Megonigal, J. P.: Moving Beyond Global Warming Potentials to
801 Quantify the Climatic Role of Ecosystems, *Ecosystems*, 18(6), 1000–1013,
802 doi:10.1007/S10021-015-9879-4/TABLES/2, 2015.

803 Nóbrega, G. N., Ferreira, T. O., Siqueira Neto, M., Queiroz, H. M., Artur, A. G.,
804 Mendonça, E. D. S., Silva, E. D. O. and Otero, X. L.: Edaphic factors controlling
805 summer (rainy season) greenhouse gas emissions (CO₂ and CH₄) from semiarid
806 mangrove soils (NE-Brazil), *Sci. Total Environ.*, 542, 685–693,
807 doi:10.1016/j.scitotenv.2015.10.108, 2016.

808 Norman, J. M., Kucharik, C. J., Gower, S. T., Baldocchi, D. D., Crill, P. M., Rayment,
809 M., Savage, K. and Striegl, R. G.: A comparison of six methods for measuring soil-
810 surface carbon dioxide fluxes, *J. Geophys. Res. Atmos.*, 102(D24), 28771–28777,
811 doi:10.1029/97JD01440, 1997.

812 Peel, M. C., Finlayson, B. L. and McMahon, T. A.: Updated world map of the Köppen-
813 Geiger climate classification, *Hydrol. Earth Syst. Sci.*, 11(5), 1633–1644,
814 doi:10.1002/ppp.421, 2007.

815 Poffenbarger, H. J., Needelman, B. A. and Megonigal, J. P.: Salinity Influence on
816 Methane Emissions from Tidal Marshes, *Wetlands*, 31(5), 831–842,
817 doi:10.1007/s13157-011-0197-0, 2011.

818 Prost, M. T., Mendes, A. C., Faure, J. F., Berredo, J. F., Sales, M. E. ., Furtado, L. G.,
819 Santana, M. G., Silva, C. A., Nascimento, I. ., Gorayeb, I., Secco, M. F. and Luz, L.:
820 Manguezais e estuários da costa paraense: exemplo de estudo multidisciplinar integrado
821 (Marapanim e São Caetano de Odivelas), in *Ecosistemas costeiros: impactos e gestão*
822 *ambiental*, edited by M. T. Prost and A. Mendes, pp. 25–52, FUNTEC and Museu
823 Paraense Emílio Goeldi, Belém, Brazil., 2001.

824 Purvaja, R. and Ramesh, R.: Natural and Anthropogenic Methane Emission from
825 Coastal Wetlands of South India, *Environ. Manage.*, 27(4), 547–557,
826 doi:10.1007/s002670010169, 2001.

827 Purvaja, R., Ramesh, R. and Frenzel, P.: Plant-mediated methane emission from an
828 Indian mangrove, *Glob. Chang. Biol.*, 10(11), 1825–1834, doi:10.1111/j.1365-
829 2486.2004.00834.x, 2004.

830 Reeburgh, W. S.: Oceanic Methane Biogeochemistry, *Chem. Rev.*, 2, 486–513,
831 doi:10.1021/cr050362v, 2007.

832 Robertson, A. I., Alongi, D. M. and Boto, K. G.: Food chains and carbon fluxes, in
833 *Coastal and Estuarine Studies*, edited by A. I. Robertson and D. M. Alongi, pp. 293–
834 326, American Geophysical Union., 1992.

835 Rocha, A. S.: Caracterização física do estuário do rio Mojuim em São Caetano de
836 Odivelas - Pa, Universidade Federal do Pará., 2015.

837 Rollnic, M., Costa, M. S., Medeiros, P. R. L. and Monteiro, S. M.: Tide Influence on
838 Suspended Matter Transport in an Amazonian Estuary, in *Journal of Coastal Research*,
839 vol. 85, pp. 121–125, Allen Press., 2018.

840 Rosentreter, J. A., Maher, D. T., Erler, D. V., Murray, R. H. and Eyre, B. D.: Methane
841 emissions partially offset “blue carbon” burial in mangroves, *Sci. Adv.*, 4(6), eaao4985,
842 doi:10.1126/sciadv.aao4985, 2018a.

843 Rosentreter, J. A., Maher, D. . T., Erler, D. V. V., Murray, R. and Eyre, B. D. D.:
844 Seasonal and temporal CO₂ dynamics in three tropical mangrove creeks – A revision of
845 global mangrove CO₂ emissions, *Geochim. Cosmochim. Acta*, 222, 729–745,
846 doi:10.1016/j.gca.2017.11.026, 2018b.

847 Roslev, P. and King, G. M.: Regulation of methane oxidation in a freshwater wetland by
848 water table changes and anoxia, *FEMS Microbiol. Ecol.*, 19(2), 105–115,
849 doi:10.1111/j.1574-6941.1996.tb00203.x, 1996.

850 Sahu, S. K. and Kathiresan, K.: The age and species composition of mangrove forest
851 directly influence the net primary productivity and carbon sequestration potential,
852 *Biocatal. Agric. Biotechnol.*, 20, 101235, doi:10.1016/j.bcab.2019.101235, 2019.

853 Salum, R. B., Souza-Filho, P. W. M., Simard, M., Silva, C. A., Fernandes, M. E. B.,
854 Cougo, M. F., do Nascimento, W. and Rogers, K.: Improving mangrove above-ground
855 biomass estimates using LiDAR, *Estuar. Coast. Shelf Sci.*, 236, 106585,
856 doi:10.1016/j.ecss.2020.106585, 2020.

857 Schmidt, M. W. I., Torn, M. S., Abiven, S., Dittmar, T., Guggenberger, G., Janssens, I.
858 A., Kleber, M., Kögel-Knabner, I., Lehmann, J., Manning, D. A. C., Nannipieri, P.,
859 Rasse, D. P., Weiner, S. and Trumbore, S. E.: Persistence of soil organic matter as an
860 ecosystem property, *Nature*, 478(7367), 49–56, doi:10.1038/nature10386, 2011.

861 Segarra, K. E. A., Schubotz, F., Samarkin, V., Yoshinaga, M. Y., Hinrichs, K. U. and
862 Joye, S. B.: High rates of anaerobic methane oxidation in freshwater wetlands reduce
863 potential atmospheric methane emissions, *Nat. Commun.*, 6(1), 1–8,
864 doi:10.1038/ncomms8477, 2015.

865 Shiau, Y.-J. and Chiu, C.-Y.: Biogeochemical Processes of C and N in the Soil of
866 Mangrove Forest Ecosystems, *Forests*, 11(5), 492, doi:10.3390/f11050492, 2020.

867 Shiau, Y. J., Cai, Y., Lin, Y. Te, Jia, Z. and Chiu, C. Y.: Community Structure of Active
868 Aerobic Methanotrophs in Red Mangrove (*Kandelia obovata*) Soils Under Different
869 Frequency of Tides, *Microb. Ecol.*, 75(3), 761–770, doi:10.1007/s00248-017-1080-1,
870 2018.

871 Sihi, D., Davidson, E. A., Chen, M., Savage, K. E., Richardson, A. D., Keenan, T. F.
872 and Hollinger, D. Y.: Merging a mechanistic enzymatic model of soil heterotrophic
873 respiration into an ecosystem model in two AmeriFlux sites of northeastern USA,

874 *Agric. For. Meteorol.*, 252, 155–166, doi:10.1016/J.AGRFORMET.2018.01.026, 2018.

875 Souza Filho, P. W. M.: Costa de manguezais de macromaré da Amazônia: cenários
876 morfológicos, mapeamento e quantificação de áreas usando dados de sensores remotos,
877 *Rev. Bras. Geofísica*, 23(4), 427–435, doi:10.1590/S0102-261X2005000400006, 2005.

878 Sparling, G. P. and West, A. W.: A direct extraction method to estimate soil microbial
879 C: calibration in situ using microbial respiration and ¹⁴C labelled cells, *Soil Biol.*
880 *Biochem.*, 20(3), 337–343, doi:10.1016/0038-0717(88)90014-4, 1988.

881 Sundqvist, E., Vestin, P., Crill, P., Persson, T. and Lindroth, A.: Short-term effects of
882 thinning, clear-cutting and stump harvesting on methane exchange in a boreal forest,
883 *Biogeosciences*, 11(21), 6095–6105, doi:10.5194/bg-11-6095-2014, 2014.

884 Valentim, M., Monteiro, S. and Rollnic, M.: The Influence of Seasonality on Haline
885 Zones in An Amazonian Estuary, *J. Coast. Res.*, 85, 76–80, doi:10.2112/SI85-016.1,
886 2018.

887 Valentine, D. L.: Emerging Topics in Marine Methane Biogeochemistry, *Ann. Rev.*
888 *Mar. Sci.*, 3(1), 147–171, doi:10.1146/annurev-marine-120709-142734, 2011.

889 Vance, E. D., Brookes, P. C. and Jenkinson, D. S.: An extraction method for measuring
890 soil microbial biomass C, *Soil Biol. Biochem.*, 19(6), 703–707, doi:10.1016/0038-
891 0717(87)90052-6, 1987.

892 Verchot, L. V., Davidson, E. A., Cattânio, J. H. and Ackerman, I. L.: Land-use change
893 and biogeochemical controls of methane fluxes in soils of eastern Amazonia,
894 *Ecosystems*, 3(1), 41–56, doi:10.1007/s100210000009, 2000.

895 Whalen, S. C.: Biogeochemistry of Methane Exchange between Natural Wetlands and
896 the Atmosphere, *Environ. Eng. Sci.*, 22(1), 73–94, doi:10.1089/ees.2005.22.73, 2005.

897 Xu, X., Elias, D. A., Graham, D. E., Phelps, T. J., Carroll, S. L., Wulschleger, S. D. and
898 Thornton, P. E.: A microbial functional group-based module for simulating methane
899 production and consumption: Application to an incubated permafrost soil, *J. Geophys.*
900 *Res. Biogeosciences*, 120(7), 1315–1333, doi:10.1002/2015JG002935, 2015.

901 Yang, S. S. and Chang, H. L.: Effect of environmental conditions on methane
902 production and emission from paddy soil, *Agric. Ecosyst. Environ.*, 69(1), 69–80,
903 doi:10.1016/S0167-8809(98)00098-X, 1998.

